

ELABORATION OF THE MICROCHIP CONCEPT WITH 3D MOVEMENT FOR LASER DIODE – OPTIC FIBER COUPLING

A. Dorogan
 Technical University of Moldova

INTRODUCTION

Precise and controllable delivery of laser beams or other guided modes to a desired location is an important topic, with telecommunications, and other general industrial applications. The most common means of obtaining such delivery is the use of large (i.e. macroscopic) mechanically controlled mirrors or lenses. While this technology is mature, it is limited by the mechanical nature of optical devices movement. Inertial properties of mechanically driven mirrors or lenses limit the speed with which steering direction can be changed. The other well-established beam steering device, the acousto-optic modulator, has a severely limited angular range [1].

In many domains as optical measurements, telecommunications, optical fibres are used. One of the most important challenges is to inject the light into the fibre. Nowadays, this is usually done either with large and expensive mechanical setups or passively aligned low cost modules, with much insertion loss [2]. The goal of a collaboration research project SCOPES IB no. 7420-1100981/1 hold in Switzerland was to develop a new low-cost active alignment system to inject the light coming from a laser diode into a monomode optical fibre with minimum losses. The presented concept models are a modification of the actual chip work also on the comb actuation effect.

1. FUNDAMENTALS

A fibre alignment system is usually composed of a source of light (in our case, a laser diode), one or more lenses and the optical fibre (fig. 1).

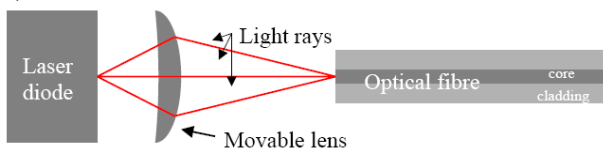


Figure 1. Schema of a fibre injection system.

The lenses are spherical and macroscopic. After a first manual alignment, the fine alignment of

the light into the fibre is carried out by moving the lens towards maximum intensity of light measured on the other side of the fibre. This is done by a feedback control loop.

1.1. Combs drive actuation

Comb drives are often used in devices with structures held by mechanical springs.

In the case of comb drives, we do not have only the force seen previously but also an additional one due to the overlap perpendicular to the displacement.

If h is the height of the device, NF is the number of fingers and g is the gap between the combs, the resulting force is:

$$F_E \approx -\epsilon_0 \epsilon_r \frac{hNF}{g} V^2, \quad (1)$$

As the elastic force of a beam is given by Eq. (2) where E is the Young's modulus, L is the length of the spring and t is its width:

$$F_E = \frac{Eht^3}{L^3} x, \quad (2)$$

The sum of the forces in the situation of Figure 2 is given by:

$$x = \frac{1}{2} \frac{\epsilon_0 \epsilon_r NF L^3}{gEt^3} V^2. \quad (3)$$

In this case, the displacement varies in function of the square of the voltage.

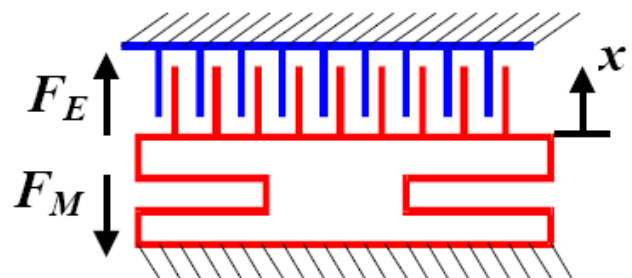


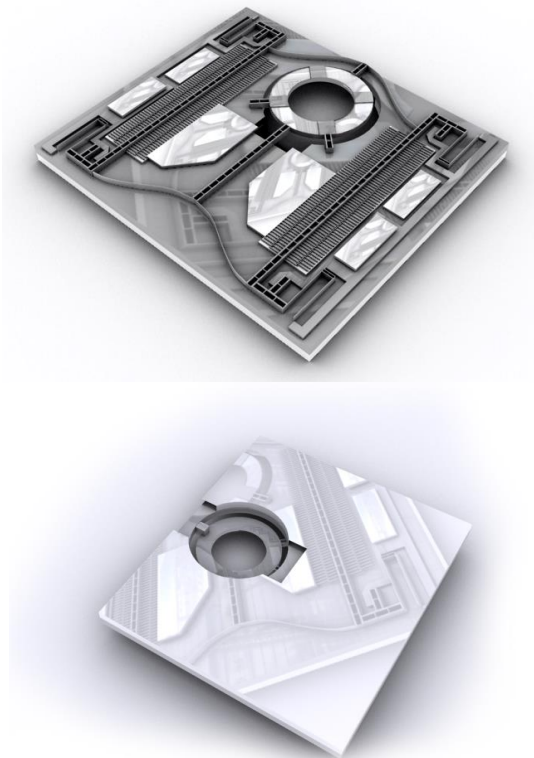
Figure 2. Schema of comb drives held by springs.

2. DESIGN

Depending on optical and packaging configurations, the design has to be adapted. In this chapter, the new design based on the novel silicon header packaging system developed at Intel will be presented.

Figure 3 shows a 3D drawing of the chip. Here are some of the construction characteristics:

- Two etching depths on front- and backside of the chip to obtain more complex 3D structures;
- Metallization on both chip sides;
- Circular platform with four small alignment structures for lens assembly;
- Focusing Lens.



b)

Figure 3. 3Ds Max image of the chip. a) - *Topside view*; b) - *Backside view*.

2.1. Circular platform

As the lens has a circular shape and in order to save space to be able to place the platform a little bit more off-centre on the chip, there was designed a circular moving frame. The size of its inner part is also being enlarged and four small alignment structures are placed on the four cardinals of the circle.

The lens intended to be assembled on the device is processed on both sides. On topside, the

lens is etched and on backside, an alignment structure of 25 μm height with inclined sidewalls to about 70° is present. The structure is made in order to facilitate the alignment and assembly of the lens on top of the MEMS platform [3].

2.2. Lens assembly

There has been made lens assembly on chips at different thermal conditions and with a different glue placement for a better lens stacking.

After a row of assembling processes there were revealed some problems with the chip's construction. The springs have been broken after the chip was placed in the oven for a better glue drying process. The temperatures used were: 80°C , 60°C and 50°C . The springs' damage was revealed at 80°C and 60°C drying. Perhaps, this happens because of the dilatation process of the material that occurs during healing. Figure 4 shows the damage consequences after a drying process. Another possible cause of damage can be the tensions applied on the chip during assembly.



Figure 4. Construction damage occurred during assembly and drying processes.

There wasn't revealed any construction damage at a healing temperature of 50°C . This means the drying process must be a slow one at a low temperature so that the chip won't be damaged during the assembly.

For a better assembling and for minimizing the damages that occur during the assembly, the glue drops are better to be positioned on the especially reserved place as shown in figure 5. This involves a better stacking of the lens on the moving surface of the chip. Figure 6 shows the assembled lens on the chip with its right positioning.

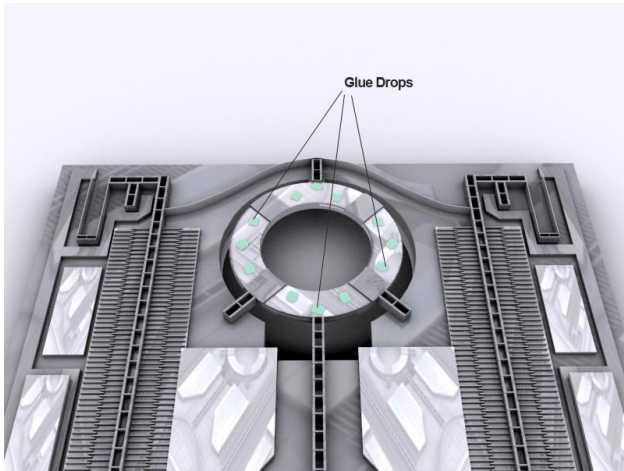


Figure 5. Glue drops positioning for a better assembly

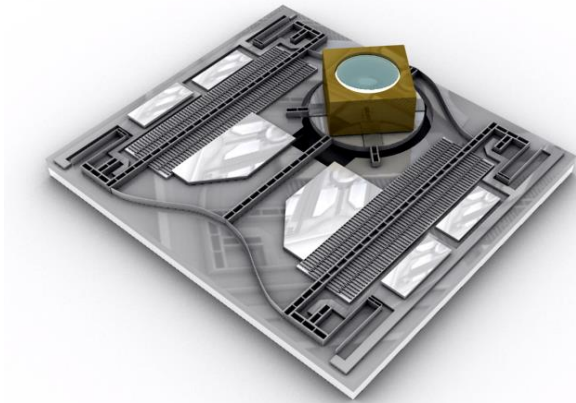


Figure 6. Assembled lens on the chip.

3. OPTICAL BEAM MEASUREMENTS AND CALCULATIONS

There was made a measurement of the optical beam that offers the possibility of determination the distance between certain objects placed in a mounted system similar to the one presented in figure 7.

The main goal was to determine the distance between the zero point of the mounted system and the focal point of the lens. This mean there was a need to determine the certain position were the optical laser beam has the minimum surface.

The main mounted system is consisted of a laser diode, a lens for collimating the laser beam and a photo detector. All the measurements were made for different positions of the photo detector. This way we obtained different widths and heights of the laser beam spot. The laser beam spot possessed different width and height at a certain

position of the photo detector. This is because of the laser diode property of emission.

FD1, FD2,... - position of the photodetector
 DL - laser diode (light source)
 F - focal point of the lens

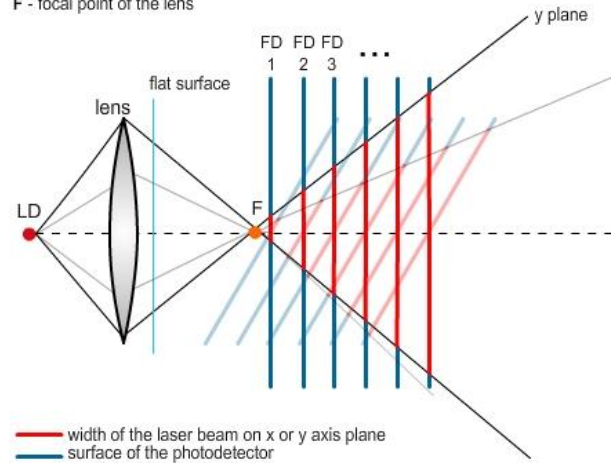


Figure 7. Mounted optical system used for measurements and calculation

There measurements that were taken are the distance between the zero point of the mounted system and the photo detector and the parameters of the spot projected on the photo detector. The main data available after measurements and additional data are presented in table 1 and 2.

Table 1. Main measurements data available.

Distance zero point – photo detector (μm)	Spot width on x plane (μm)	Spot width on y plane (μm)
50000	4752	5825
52500	4142	4973
55000	3378	4130
57500	2651	3253
60000	1926	2357
61000	1645	1998
62000	1354	1645
62500	1226	1468

Table 2. Additional available data.

Distance laser diode – lens (μm)	327
First surface	flat
Lens thickness (μm)	550
Lens diameter (μm)	500
Lens radius of curvature	900, $k=-3.3$

Calculations:

Lens focal point. The lens focal point was calculated from the relation shown below:

$$f = \frac{R_{curv}}{n_{Si} - 1} = \frac{900}{3,6 - 1} = 346,15 \mu m, \quad (4)$$

where:

n_{Si} - refractive index of the lens (material Si), R_{curv} - radius of lens' curvature.

Determination of the distance between the focal point – zero point and the distance of the focal point – the photo detector's position of the mounted system. For determination of the distance between the focal point and the zero point of the mounted system it was necessary to determine the distance between the focal point and each of the photo detector's position. For this necessity it is necessary to determine the angle between the main axis of the laser beam's propagation and the extremity of the spot width (angle θ). The main calculation method is shown in figure 8.

The d distance is the difference of the semi width of the two neighbour spots of two positions of the photo detector:

$$d = c - b, \quad (5)$$

where c , b - semi width of two neighbour spot widths.

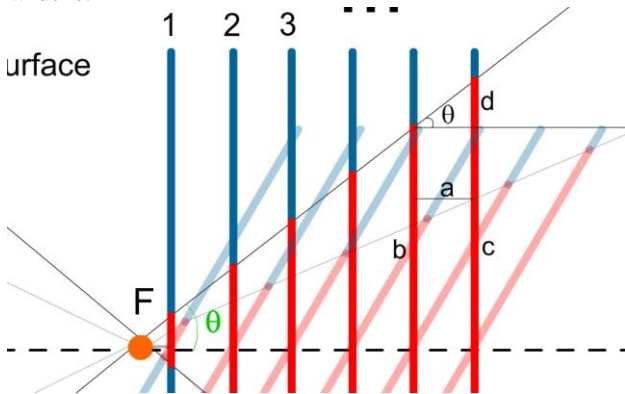


Figure 8. Determination of the θ angle

The distance a is the difference between two positions of the photo detector. The determination of the θ angle is made with the help of the following relation:

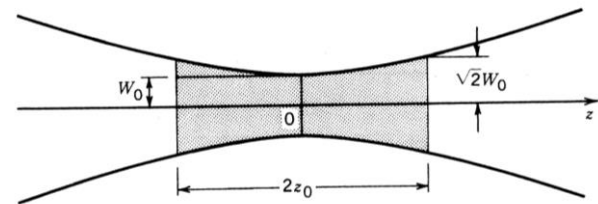


Figure 9. The depth of focus of a Gaussian beam

$$tg \theta = \frac{d}{a}. \quad (6)$$

The θ angle was determined from the difference of each two neighbour positions of the photo detector and there was calculated the arithmetic media between all the values. We obtained the medium angle θ :

$$\theta = 0.10018309$$

- for the calculations made on the x plane

$$\theta = 0.123472147$$

- for the calculations made on the y plane

The determination of the distance between the focal point and each position of the photo detector (let us name it x) is determined by the following relation:

$$tg \theta = \frac{b}{x}. \quad (7)$$

Then:

$$x = \frac{b}{tg \theta}, \quad (8)$$

(for the photo detector's position 5, fig. 8).

This formula was used for each distance of the photo detector's position.

After the determination of the x distance, the distance between the zero point of the mounted system and the focal point, photo detector position – focal distance and lens – zero point were determined.

While working with a Gaussian beam we must take into the account the focal depth of the lens. The θ angle can not be determined geometrically in this region because the optical beam surface increases as a nonlinear function. After this certain distance the calculus is rather easy and it can give quite true results. But the most real results are achieved if the calculations would be made as near as possible to the focal depth region.

In either direction, the beam gradually grows “out of focus.” The axial distance within which the beam radius lies within a factor $\sqrt{2}$ of its minimum value (i.e., its area lies within a factor of 2 of its minimum) is known as the depth of focus or confocal parameter (Fig. 9).

The depth of focus is twice the Rayleigh range,

$$2z_0 = \frac{2\pi W_0^2}{\lambda}. \quad (9)$$

The depth of focus is directly proportional to the area of the beam at its waist, and inversely proportional to the wavelength. Thus when a beam is focused to a small spot size, the depth of focus is short and the plane of focus must be located with greater accuracy. A small spot size and a long depth of focus cannot be obtained simultaneously unless the wavelength of the light is short. For $\lambda = 633 \text{ nm}$ (the wavelength of a He — Ne laser line), for example, a spot size $2W_0 = 2 \text{ cm}$ corresponds to a depth of focus $2z_0 = 1 \text{ km}$. A much smaller spot size of $20 \mu\text{m}$ corresponds to a much shorter depth of focus of 1 mm .

The first four results that express the distance between the focal distance and the photo detector are quite satisfying. The rest show that the measurement was taken in the region of a nonlinear function. And the distance between the zero point and the focal distance differs on a big amount which is not a satisfying result. For a restricted $10 \mu\text{m}$ beam width the calculated result of the focal depth is $2z_0 = 858,7786 \mu\text{m}$.

For achieving better results and precise values the distance between the focal point and the photo detector position must be determined for each calculated θ angle.

Here we obtained good results, but also, it was evident that the first four values a real and the rest ones are not satisfying values (nonlinear region increase of the beam width).

With these already calculated results we can also determine the magnitude of the lens, the distance between the zero point and each of the optical system's components.

4. 3D MOVEMENT CONCEPT (INTEGRATED Z AXIS)

The z-alignment is very important in the final packaging. Indeed, if the distance varies of five microns from the optimal position, the graph shows that the fibre has to be moved of several hundreds of microns. In this case, the maximal theoretical coupling efficiency drops to about sixty percent [5].

The actual lens dimensions differ from those represented in figure 10. The packaging alignment is not as critical in the plane perpendicular to the optical axis. If a misalignment occurs between the diode, the lens and the fibre, it can be compensated by moving the platform. This graph shows that the coupling efficiency is about

the same after position compensation with the MOPOS chip [5].

There have been made some tries of construction modelling with the purpose of introducing a Z axis movement, so that the problem with the packaging and optical setup could be solved.

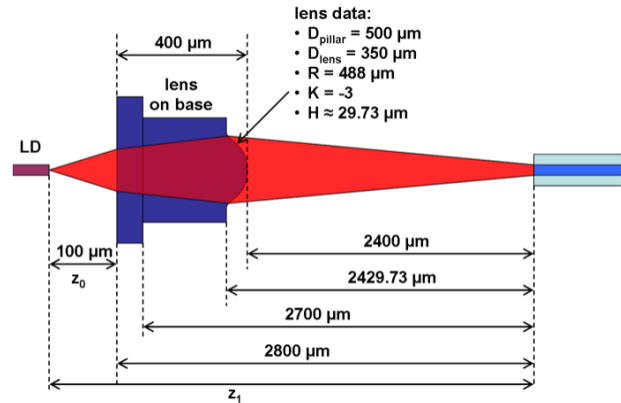


Figure 10. Schematic view of the optical setup.

Of course, this involves some construction changes, and also this requires some changes of the fabrication technology.

The first construction model concept that was first designed with a special software 3Ds max is represented in figure 11.

Our suggestion was not to change very much the actual construction of the chip. In this case we added a third actuator which will provide a Z axis movement of the platform. The actuator was placed perpendicularly to the other ones so that it could move the two springs that are holding the moving platform.

After studying this construction, it was evident, that the current fabrication technology would not be enough to provide the construction and the position of the springs. In this case we will need a multilayer technology of fabrication. Of course, if we would use such a technology this model can be discussed further. And there can be done some tries of its fabrication.

In this construction, the two springs are moving a second platform that responds for the Z axis lift. The first platform is used for the X and Y movement. The second platform must be held by three vertical bars so that the second platform won't be displaced during the movement process.

Thinking about a model that can be better adjusted to the fabrication technology used for fabricating the actual chip (without any Z axis movement) we tried to model a second construction of the chip with an integrated Z axis movement shown in figure 12.

In this case we added two more actuators that will provide a movement in the same plane as

the other ones do (X plane). The movement of the both actuators must be opposite one to another one. This way we obtain the movement effect that we need. These two actuators are holding two pieces that have a special shape and form. Figure 7 shows the shape of the two pieces that provide a Z axis movement.

The shape was modelled so that if the movement of the pieces is opposite to each other, the platform that is placed upon them should move upwards and downwards (along the Z axis).

The metal contacts have the same shape and form as it is at the other actuators. Of course, if we discuss the possibility of integrating this system on the same chip (with the same dimensions) this means that the added actuators must have smaller dimensions so that they could fit the actual construction of the chip. But we think that the best construction is the one with an increased x axis dimensions. Taking into the account the fabrication technology this construction is quite hard to be done. A possible way to be done is to fabricate it in several phases.

The first phase is probably the main chip construction. After that, there could be fabricated the actuators that provide the two pieces movement on a separate wafer so that it could be bonded after with the first structure. The third phase would be the lens gluing on the platform and after that its mounting after a bonding of the holding bars that provide a stability of the platform while moving.

Of course, this involves a row of complex technology processes, among them some that can be hardly done to adjust the construction shown above.

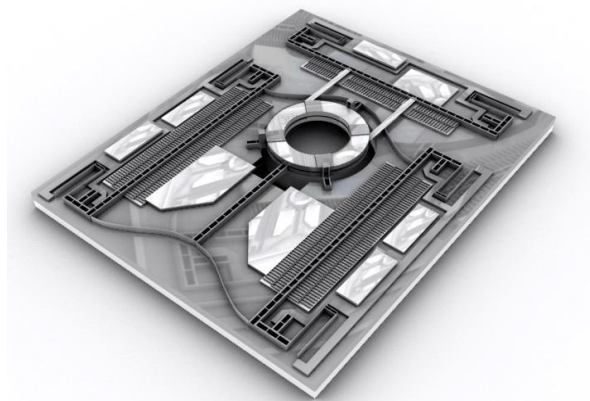
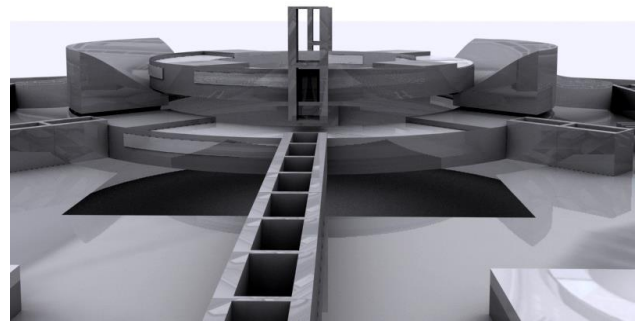


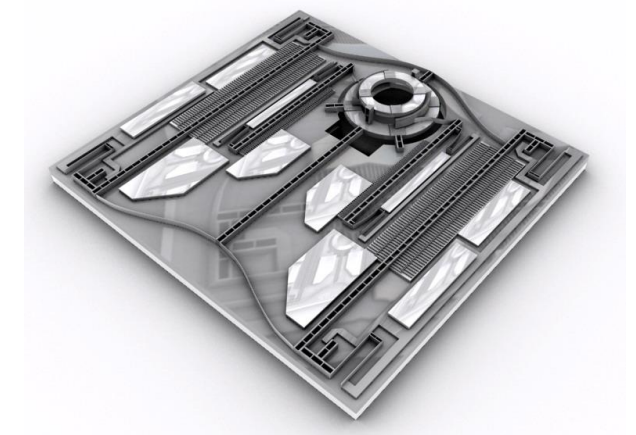
Figure 11. 3D concept of an integrated Z axis on the chip.

The presented two concept models are of a big interest for the development of the actual communication systems, especially for using them in an optic module for coupling the optic fibre with the laser diode and the integrated Z axis would give a great possibility of improving the characteristics

and the properties of the coupling modules of an fibre optic communication system.



a)



b)

Figure 12. a) - Shape of two pieces providing a Z axis movement to the platform; b) - Second 3D concept with opposite actuators

Bibliography

1. **Dr. Philip J. Bos.** *Beam Steering.* <http://www.Icl.kent.edu/boslab/>, (2002).
2. **Newport.** *Modular Alignment System for Photonics Packaging.* <http://www.newport.com/store/product.asp?id=4433>.
3. **Petremand Y.** *Mopos annual report 2004// Annual report, IMT, January 2004.*
4. **Epitoux M., Petremand Y., Noell W., De Rooij N., and Verdiell J.-M.** *Silicon optical benches for next generation optical packaging: Going vertical or horizontal? // IEEE 2005, Electronic Components and Technology Conference, pag. 1339-1342, 2005.*
5. **Petremand Y.** *Mopos annual report 2005// Annual report, IMT, February 2005.*
6. **Petremand Y.** *Mopos annual report 2006// Annual report, IMT, February 2006.*

Recomandat spre publicare: 14.05.2007.